Fundamental diagram in the context of the Social Force Model

I.M. Sticco, G.A. Frank, F.E. Cornes, and C.O. Dorso
Departamento de Física, Facultad de Ciencias Exactas y Naturales,
Universidad de Buenos Aires, Pabellón I, Ciudad Universitaria, 1428 Buenos Aires, Argentina.
Unidad de Investigación y Desarrollo de las Ingenierías,
Universidad Tecnológica Nacional, Facultad Regional Buenos Aires,
Av. Medrano 951, 1179 Buenos Aires, Argentina. and
Instituto de Física de Buenos Aires, Pabellón I,
Ciudad Universitaria, 1428 Buenos Aires, Argentina.
(Dated: November 3, 2018)

PACS numbers: 45.70.Vn, 89.65.Lm

I. INTRODUCTION

$$J = v(\rho)\rho \tag{1}$$

II. BACKGROUND

A. The Social Force Model

Our research was carried out in the context of the "social force model" (SFM) proposed by Helbing and coworkers [**?**]. This model states that human motion is caused by the desire of people to reach a certain destination, as well as other environmental factors. The pedestrians behavioral pattern in a crowded environment can be modeled by three kind of forces: the "desire force", the "social force" and the "granular force".

The "desire force" represents the pedestrian's own desire to reach a specific target position at a desired velocity v_d. But, in order to reach the desired target, he (she) needs to accelerate (decelerate) from his (her) current velocity $\mathbf{v}^{(i)}(t)$. This acceleration (or deceleration) represents a "desire force" since it is motivated by his (her) own willingness. The corresponding expression for this forces is

$$\mathbf{f}_d^{(i)}(t) = m_i \, \frac{v_d^{(i)} \, \mathbf{e}_d^{(i)}(t) - \mathbf{v}^{(i)}(t)}{\tau} \tag{2}$$

where m_i is the mass of the pedestrian i. $\mathbf{e}_d$ corresponds to the unit vector pointing to the target position and τ is a constant related to the relaxation time needed to reach his (her) desired velocity. Its value is determined experimentally. For simplicity, we assume that v_d remains constant during an evacuation process and is the same for all individuals, but $\mathbf{e}_d$ changes according to the current position of the pedestrian. Detailed values for m_i and τ can be found in Refs. [**? ?**].

The "social force" represents the psychological tendency of two pedestrians, say i and j, to stay away from each other by a repulsive interaction force

$$\mathbf{f}_s^{(ij)} = A_i \, e^{(r_{ij} - d_{ij})/B_i} \mathbf{n}_{ij} \tag{3}$$

where (ij) means any pedestrian-pedestrian pair, or pedestrian-wall pair. A_i and B_i are fixed values, d_{ij} is the distance between the center of mass of the pedestrians i and j and the distance $r_{ij} = r_i + r_j$ is the sum of the pedestrians radius. $\mathbf{n}_{ij}$ means the unit vector in the $\vec{ji}$ direction.

Any two pedestrians touch each other if their distance d_{ij} is smaller than r_{ij}. In this case, an additional force is included in the model, called the "granular force". This force is considered be a linear function of the relative (tangential) velocities of the contacting individuals. Its mathematical expression reads

$$\mathbf{f}_g^{(ij)} = \kappa \, (r_{ij} - d_{ij}) \, \Theta(r_{ij} - d_{ij}) \, \Delta\mathbf{v}^{(ij)} \cdot \mathbf{t}_{ij} \tag{4}$$

where κ is a fixed parameter. The function $\Theta(r_{ij} - d_{ij})$ is zero when its argument is negative (that is, $r_{ij} < d_{ij}$) and equals unity for any other case (Heaviside function). $\Delta\mathbf{v}^{(ij)} \cdot \mathbf{t}_{ij}$ represents the difference between the tangential velocities of the sliding bodies (or between the individual and the walls).

The above forces actuate on the pedestrians dynamics by changing his (her) current velocity. The equation of motion for pedestrian i reads

$$m_i \, \frac{d\mathbf{v}^{(i)}}{dt} = \mathbf{f}_d^{(i)} + \sum_{j=1}^{N} \mathbf{f}_s^{(ij)} + \sum_{j=1}^{N} \mathbf{f}_g^{(ij)} \tag{5}$$

where the subscript j represents all the other pedestrians (excluding i) and the walls.

B. Fundamental Diagram

III. NUMERICAL SIMULATIONS

IV. RESULTS

A. Fundamental diagram in the original model

In Fig 1, we show the fundamental diagram (density vs. flow) for different corridor widths. We can distinguish the two typical branches of the fundamental diagram. In the free flow branch ($\rho < 5$), the flow increases linearly with the density, since there are no collisions between pedestrians. In this regime, pedestrians achieve the desired velocity, leading to a flow that grows linearly with the density. That is reason why the flow takes the value of $J \sim \rho$ until $\rho = 5$. This behavior applies to all the corridor width analyzed.

On the other hand we have the congested branch for $\rho > 5$. Here we face two different scenarios:

- i) In narrow corridors (say $w < 10$) we can see that the flow reduces as the density increases. This resembles the traditional behavior of the fundamental diagram reported in the literature.
- ii) In wide corridors (say $w > 15$) we see that the flow increases with density. This contradicts the typical behavior of the fundamental diagram.

We wonder what is the reason that determines the increase or decrease of the flow in the congested branch. Since the trajectories of pedestrians are straight (there are no crossing path that could reduce the flow), we can assert that the the friction force is the only factor in the flow reduction. The inset of the Fig. 1 corresponds to the empirical measures of Helbing et al. at the entrance of the Jamaraat bridge (the corridor with was $w = 22$ m). Notice that our simulated result corresponding to a $w = 22$ m corridor, exhibit a different behavior in the congested branch. In the simulated case, the flow increases even for the greatest densities. On the contrary, the empirical measurement exhibit a flow reduction for $\rho > 5$ and it reaches a plateau for the highest density values.

In order to satisfy the fundamental diagram reported in the literature, It is necessary that the flow at the maximum density ($\rho_{max} = 9$) be less than the flow at $\rho = 5$. That is: $J(\rho = 9) < J(\rho = 5)$. From the flow definition in Eq. 1 we can derive

$$v(\rho_{max}) < \frac{5 v_d}{\rho_{max}}$$
$$v(\rho_{max}) < \frac{5}{9} v_d$$

As our desired velocity is fixed $v_d = 1$ m/s, we conclude that the speed at the maximum density has to be bounded by $v(\rho_{max}) \lesssim 0.5$ m/s in order to satisfy the qualitative behavior of the fundamental diagram reported in the literature.

The above reasoning is consistent with the speed-density results shown in Fig. 2.As a visual guide we plotted $v = 0.5$ m/s with a dashed line. Pay attention to the speed values in $\rho_{max} = 9$. The values corresponding to the wider corridors ($w = 15$ m and $w = 22$ m) both exceed $v = 0.5$ m/s. Otherwise, the values corresponding to narrower corridors fall below $v = 0.5$ m/s.

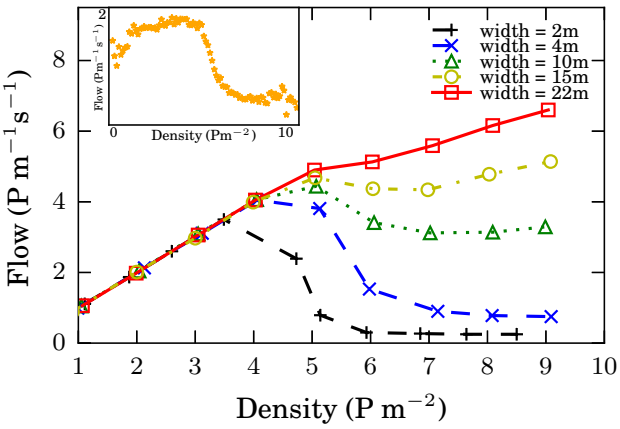

FIG. 1: Flow as a function of the density for different widths. Initially, pedestrians were randomly distributed along the corridor. The measurements were taken in the middle of the corridor once the system reached the stationary state. The length of the corridor was 28 m in all cases with periodic boundary conditions in the x direction.

The plots in Fig.2 support the fact that when the density is low enough, pedestrians manage to walk at the desired velocity ($v = 1$ m/s). Only for $\rho > 5$ the velocity begins the slow down proses. The inset shows the measurements at the entrance of the Jamaraat bridge. When comparing our results with the measurements of the Jamaraat bridge, it must be pointed out that the latter do not show a constant velocity for lower densities. We attribute this difference to the fact that in the real system, the pedestrian path are more complex when the density low. Another interesting finding here is that the wider the corridor, the greater the velocity for all the density values. In Section IV B we will further discuss this topic.

B. Velocity profile

As we mentioned in Section IV A, when the density is low, pedestrians achieve the desired velocity ($v = v_d = 1$ m/s). Since this result is only valid for the area located in the middle of the corridor, we want to shed some light and understand what is happening in the entire corridor. In Fig. 3 we show the velocity profile (velocity vs.

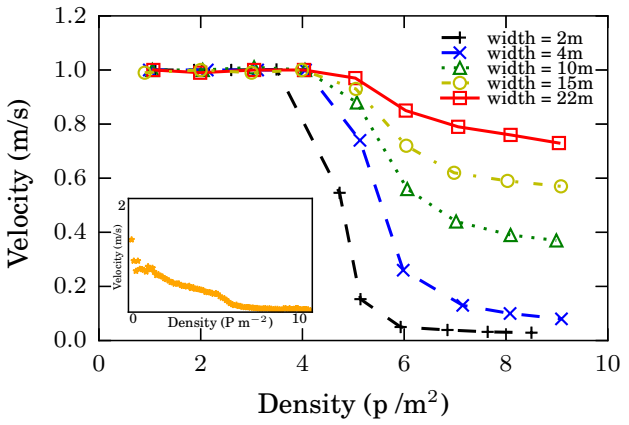

FIG. 2: Speed as a function of the density for different widths. Initially, pedestrians were randomly distributed along the corridor. The measurements were taken in the middle of the corridor once the system reached the stationary state. The length of the corridor was 28 m in all cases with periodic boundary conditions in the x direction.

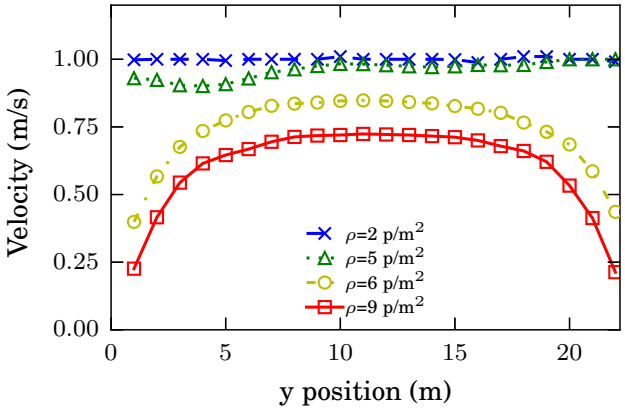

FIG. 3: Velocity profile (velocity vs y-position) for different densities (see legend for the corresponding densities). The simulated corridor was 28 m lenght. Pedestrians walk from left to right with periodic boundary condition in the x-direction. Initially, pedestrians were randomly distributed, the corridor width was $w = 22\ m$ in all the cases.

y-location) of the pedestrians in the corridor. We can see that low-density situations lead to a cruising velocity profile $v = v_d$. This is valid for every location in the corridor (not only the center as was previously discussed). For higher densities, the velocity profile turns into to a parabola-like function that resembles the typical velocity profile under conditions of the laminar flow in a viscous fluid, where the velocity increases toward the center of a tube. In our case, pedestrians near near the walls are the one with the lower velocity. The velocity increases when moving away from the wall until it reaches the maximum in the center of the corridor. This behavior suggests that the friction that the wall exerts on pedestrians, is playing a fundamental role in the velocity distribution. We did some simulations removing the walls and adding periodic boundary conditions in the y-coordinate. This yield to constant-cruising speed profiles for all the densities, confirming that the walls are a necessary condition in order to produce a parabola-shaped speed profile.

In Fig. 4 we show the velocity profile for different widths. The x-axis of the plot corresponds to the y-location normalized by the width of the corridor. The density chosen was $\rho = 6$ since we wanted to study a situation in which pedestrians collide with each other, remember that when $\rho < 5$ pedestrians manage to avoid collisions. We can see the parabola shape in which lower velocities are located in the areas near the walls. There is a clear dependence of v_{max} and the corridor width. It is interesting that the wider the corridor, the higher the maximum velocity value reached. The inset of the figure shows the same data normalized by the maximum speed value correspondent to each corridor width. Notice that once normalized, all the data follow the same pattern. This suggests that regardless the scale of the corridor, the speed profile exhibit a fundamental behavior. This means that, the velocity growth rate from the wall towards the center of the corridor, is the same regardless of the size of the corridor

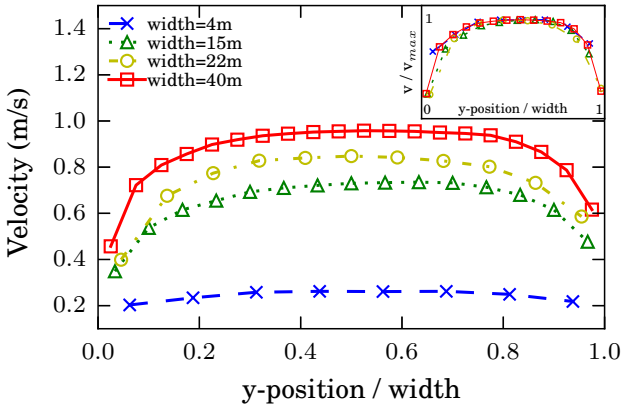

FIG. 4: Velocity profile (velocity vs y-position) for different corridors width (see legend for the corresponding widths). The simulated corridor was 28 m length. Pedestrians walk from left to right with periodic boundary condition in the x-direction. Initially, pedestrians were randomly distributed, the density was $\rho = 6$ in all the cases. The inset shows the same data with velocity normalized by the maximum value corresponding to each dataset.

C. Work done by friction force

We have shown how the velocity takes different values along the corridor. We also analyzed the work done by the friction between pedestrians in the corridor. The work exerted was numerically calculated for each pedestrian with the Simpson rule. The integration step was $\Delta t = 0.05$ s. Once all the pedestrians had its work calculated, we proceed to create a squared grid in the corridor. The cells were 1 m length, and we associated the work on the pedestrians to the cell where they were placed. In Fig. 7 we show three heat maps of the absolute value of the work done by the pedestrian-pedestrian friction force. The axis represent the x location and y location of the corridor. The heat map denotes higher work for red color and lower work for the blue color. The walls are located at $y = 0$ and $y = w$ (bottom and top of each figure). Fig. 7d corresponds to a 10 m width corridor, Fig. 7e corresponds to a 15 m width corridor and Fig. 7d corresponds to a 22 m width corridor.

In the three figures we observe the same pattern: the regions near the walls (bottom and top) are the regions in which pedestrians suffer the higher work done by the friction. In the center of the corridor the work is reduced in all the cases. Another interesting observation is that the work seems to increase with the corridor width. This happens because in the wide corridors the relative velocity between pedestrians is greater. See Fig. 4 and compare the slopes between the parabolas. It can be seen that the wider the corridor, the greater the slope (corresponding to locations near the wall). As it is stated in Eq.(4), the friction force depends on the compression and the relative velocity among pedestrians. The differences between Figs. 7d, 7e and 7f are only explained by the increment of the relative velocity. The compression levels remain the same in the three cases since the compression only depends on the density (which is fix at $\rho = 6$ for the three figures).

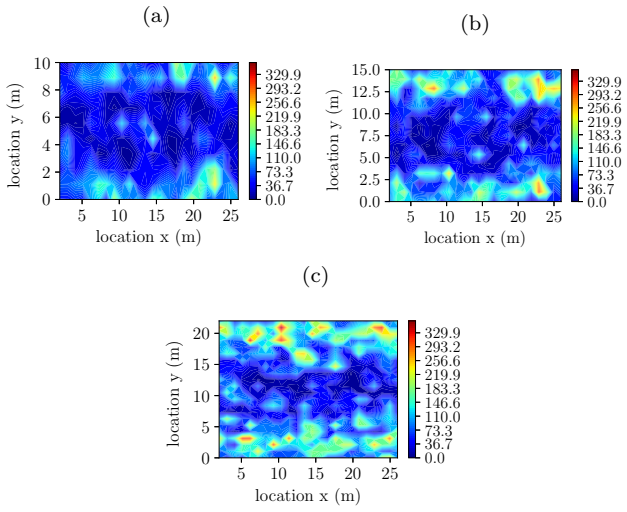

FIG. 5

D. Friction modification

As already mentioned, the results shown so far indicate that friction may be the key to improving the fundamental diagram. We want to make clear that improving the fundamental diagram means obtaining the congested branch reported by different authors, in particular in the Jamaraat study of Helbing et al. where the congested branch reaches a plateau in a 22 m width corridor. The original version of the Social Force Model proposes the same friction coefficient for the pedestrian-pedestrian interaction and the pedestrian-wall interaction. The value proposed was $\kappa = 2.4 \times 10^4$. This value is widely used by the pedestrian dynamics community despite it lacks a rigorous foundation.

We tested how the system reacts to the modification of the friction value. Fig. 6 shows the flow vs density for different friction values. The triangles correspond to the increment of the wall friction in one order of magnitude (now $\kappa_w = 2.4 \times 10^5$). In this case we left the pedestrian-pedestrian friction unchanged. We can see that the flow reduces a little bit, but this is not enough to produce the negative slope that characterizes the congested regime.

The circles correspond to a modification of the friction between pedestrians without changing the value of the wall friction. We increased the pedestrian-pedestrian friction by a factor of ten ($\kappa_i = 2.4 \times 10^5$). Here we see a significant reduction of the flow. The qualitative behavior resembles the fundamental diagram reported by Helbing et al. with a well defined congested branch for the greatest densities.

We also tested the case were both friction coefficients are ten times the value of the original model (now $\kappa_w = \kappa_i = 2.4 \times 10^5$). The squared symbols represent this scenario. As expected, the flow reduces significantly respect the original case (cross symbol plot). Interestingly, the reduction of the flow is more than the reduction due to the increment of κ_i plus the reduction of the flow due to κ_w. This behavior is indicative that the superposition principle does not hold in this system. This phenomena is explained by the non-linearity of the equation of motion.

This finding allows us to affirm that the friction plays a crucial role in the functional behavior of the fundamental diagram. The increment of both individual-individual friction and wall friction are determinant in order to achieve a congested branch. Other authors attain the congested branch modifying different aspects of the model. Parisi et al. impose zero desired velocity once pedestrians are close enough **??**, Johannson increases the relaxation time in order to slow down the net-time headway **??** and more recently, Kwak et al.**??** induce the jamming transition by an attraction. Our results show that the empirical behavior for the fundamental diagram can be achieved by properly increasing the friction coefficients. In appendix we discuss about how the modification of the relaxation time and the increment of the friction coefficient yield the same effect, since they affect the same term in the reduced-in-units equation of

motion.

We argue that in real scenarios, a combination of all these factors may be the cause of the marked flow reduction that portray the fundamental diagram. The pedestrian's path can be very complex even if it is a simple enclosure (straight corridor) and the target is well defined (unidirectional flow). Beyond the complexities given by the internal motivations of pedestrians, we strongly suggest studying and modeling coefficients of friction between individuals and friction with the walls. These two parameters have shown to be very important in the dynamics and deserve a closer inspection in future research.

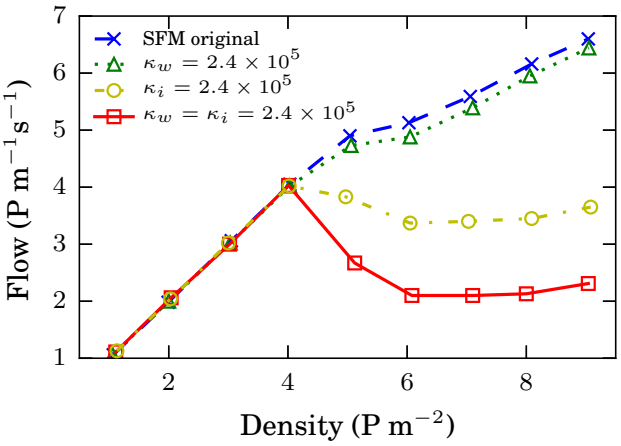

FIG. 6: Fundamental diagram (flow vs density) for different friction coefficient (see legend for the corresponding values). The simulated corridor was 28 m length. Pedestrians walk from left to right with periodic boundary condition in the x-direction. Initially, pedestrians were randomly distributed. For each density we measure the flow once the system reaches the stationary state.

E. Clusters

Cluster formation is a very importan process in pedestrian dynamics. Moreover, is the key procces that explains the clogging phenomena in bottleneck evacuations. We analyzed the clustering formation according to the granular cluster definition given in In Fig. IV E we show the cluster size distribution for three different densities: For each density we studied the case in which kw and ki are both one order of magnitud higer than the original model (these correspond to the righ hand plot). For comparison reasons we also present the

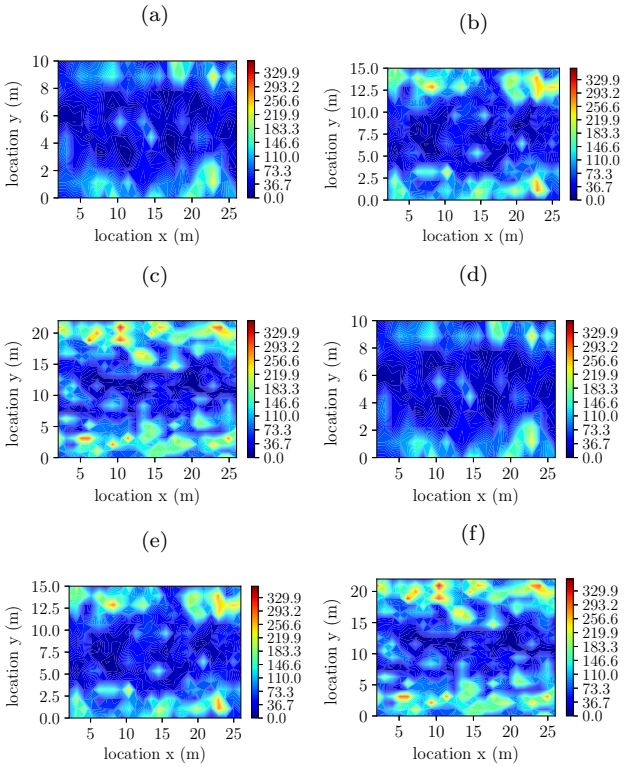

FIG. 7

V. CONCLUSIONS

ACKNOWLEDGMENTS

This work was supported by the National Scientific and Technical Research Council (spanish: Consejo Nacional de Investigaciones Científicas y Técnicas - CONICET, Argentina) grant number PIP 2015-2017 GI, founding D4247(12-22-2016).

Appendix A: